

Analysis and Design of Whole-Head Magnetic Brain Stimulators: A Simulation Study

Chany Lee, Chang-Hwan Im*, and Hyun-Kyo Jung

Abstract: This paper proposes a helmet-type whole-head brain stimulator system considering a realistic head geometry. For more accurate design and computer simulations, a realistic volume conductor model was adopted and the current evoked on human cerebral cortex was analyzed using the boundary element method (BEM). To obtain a more focalized evoked current around the target points, various coil configurations were tested and an average targeting error of about 10 mm was obtained.

Keywords: Boundary element method (BEM), inverse problem, realistic volume conductor, transcranial magnetic stimulation (TMS).

1. INTRODUCTION

It is well known that external stimulations with a time varying magnetic field can induce electrical currents in conductive neural or muscular tissues [1-6]. Early studies on magnetic stimulation used a single ring-type or eight-figured coil [1-3], but recently multi-channel magnetic stimulation has been widely studied [4-6]. Using multiple independently controlled stimulating coils, one can stimulate multiple loci simultaneously, or with a short delay between the pulses. The operator can also alleviate the nuisance caused by the activation of undesired structures by suppressing the field at selected locations. Moreover, it is possible to quickly scan the various brain regions since the coils need not to be moved during scanning. The use of multiple coils improves the mapping resolution, since the stimulating field can be made more concentrated [4]. In previous studies, multi-channel stimulations were applied not only to peripheral nerves [4,5], but also to brain cortical neurons [6], which is especially called transcranial

magnetic stimulation (TMS). TMS has many clinical or neuroscience applications because it is less invasive and less painful than electrical brain stimulation techniques [3,7]. It can be used to verify the functions of specific brain regions or to control human actions. Previous studies have shown that TMS is also promising for curing neuropsychiatric or central-nervous-system diseases, such as depression, Parkinson's disease, epilepsy, and so on [7].

Previous studies on multi-channel magnetic stimulation, however, utilized simple coil configurations such as planar and semi-spherical arrangements. Moreover, simple head models such as free-space or cylindrical conductor models were used to evaluate the evoked electric field inside the conductive tissues [4-6]. In the present study, we propose a helmet-type whole-head TMS system considering the realistic head model, for the first time. Various coil configurations and coil shapes were simulated using the boundary element method (BEM) with realistic volume conductor models extracted from structural magnetic resonance (MR) images, and the results were compared by adopting a novel concept named an error map. From these simulation studies, the most appropriate coil configurations were obtained, thereby yielding enhanced targeting accuracy.

2. FIELD CALCULATION AND HEAD MODEL

TMS can be regarded as an inverse process of magnetoencephalography (MEG), which is a popular noninvasive brain mapping technique that reconstructs the brain electrical sources on the human cerebral cortex using external magnetic field recordings [8]. We calculated the TMS-evoked current on the cortex based on the well-known reciprocal relationship between MEG and TMS [4,5].

Manuscript received April 3, 2006; revised December 5, 2006; accepted February 5, 2007. Recommended by Editorial Board member Moon Ki Kim under the direction of Editor Jin Young Choi. This work was supported in part by a grant of the Korea Health 21 R&D project, Ministry of Health and Welfare, Korea (02-PJ3-PG6-EV07-0002) and in part by the project of Ministry of Commerce, Industry and Energy, Korea.

Chany Lee and Hyun-Kyo Jung are with the School of Electrical Engineering and Computer Science, Seoul National University, San 56-1, Sillim-dong, Kwanak-gu, Seoul 151-744, Korea (e-mails: chany@elecmech.snu.ac.kr, hkjung@snu.ac.kr).

Chang-Hwan Im is with the Department of Biomedical Engineering, Yonsei University, 234 Maeji-ri, Heungdeopmyeon, Wonju-si, Kangwon-do 220-710, Korea (e-mail: ich@yonsei.ac.kr).

* Corresponding author.

2.1. Formula and method

Based on the reciprocity between MEG and TMS, the relationship between the evoked electric field, E , and the external time-varying coil currents can be defined as follows [4,6]:

$$\vec{E}(\vec{r}) = -\sum_{i=1}^n (dI_i / dt) L_i(\vec{r}), \quad (1)$$

where n is the number of coils, \vec{r} is the point used to calculate the evoked electric field, dI_i / dt is the derivative of the current in the i -th coil with respect to time, and L_i is the i -th array of the lead field matrix, L , which relates the point sources to the magnetic sensors used in MEG [8]. The lead field matrix can be evaluated by calculating the magnetic flux density at a sensor position induced by a point dipolar source with unit strength. If we assume an intended (or projected) evoked field pattern, the optimal time-varying currents can be determined by solving a linear inverse problem using the minimum norm estimation (MNE) method [4] as follows:

$$dI / dt = -L^+ \mathbf{P}, \quad (2)$$

where L^+ is the pseudo-inverse of the lead field matrix and \mathbf{P} is the assumed evoked field pattern, which is defined as a $3N \times 1$ matrix, where N is the number of tessellated cortical surface meshes (refer to the next section) and '3' represents the directions of the assumed electric field vector. Then, the evoked electric field at \vec{r} can be expressed as

$$\vec{E}(\vec{r}) = -\sum_{i=1}^n (L^+ \mathbf{P})_i L_i(\vec{r}). \quad (3)$$

2.2. Realistic head models

As stated previously, conventional studies on multi-channel magnetic stimulation systems assumed simple conduction models such as a free-space or simplified volume conductor model [4-6]. In this paper, we used the boundary element method (BEM) to calculate the forward solutions and construct the lead field matrix, thereby allowing for a more realistic volume conduction effect. It has frequently been reported that considering the inner skull boundary is sufficient for the MEG forward calculations, because of the skull insulation effect [9,10]. The magnetic field at a given point \vec{r} can be obtained from (4)-(7).

$$\vec{B}(\vec{r}) = \vec{B}_\infty(\vec{r}) + \frac{\mu_0}{4\pi} \sum_{i=1}^m (\sigma_i^- - \sigma_i^+) \cdot \int_{S_j} V(\vec{r}') \frac{\vec{r} - \vec{r}'}{|\vec{r} - \vec{r}'|^3} \times d\vec{S}_j, \quad (4)$$

$$\vec{B}_\infty(\vec{r}) = \frac{\mu_0}{4\pi} \int_G \vec{j}^p(\vec{r}') \times \frac{\vec{r} - \vec{r}'}{|\vec{r} - \vec{r}'|^3} dv', \quad (5)$$

$$V(\vec{r}) = \frac{2}{\sigma_i^- + \sigma_i^+} V_\infty(\vec{r}) - \frac{1}{2\pi} \sum_{i=1}^m \frac{\sigma_i^- - \sigma_i^+}{\sigma_i^- + \sigma_i^+} \int_{S_i} V(\vec{r}') \frac{r - r'}{|\vec{r} - \vec{r}'|^3} \cdot d\vec{S}_i, \quad (6)$$

$$V_\infty(\vec{r}) = \frac{1}{4\pi} \int_G \vec{j}^p(\vec{r}') \cdot \frac{\vec{r} - \vec{r}'}{|\vec{r} - \vec{r}'|^3} dv', \quad (7)$$

where, σ_i^- and σ_i^+ are the conductivities inside and outside the i -th boundary surface S_i , respectively, and $\vec{j}^p(\vec{r}')$ is the primary current in a source space G . The magnetic field induced by the primary current can be evaluated using the electric potential V at all boundary nodes after solving (6) with the BEM. The boundary surface was extracted from high-resolution MRI data and was composed of 1016 elements and 510 nodes.

On the other hand, we restricted the locations of the target points only on the interface between the white matter and gray matter of the subject's cerebral cortex. This constraint is physiologically plausible and practical, because most neurons are located on the cortical surface (actually within a very thin region of gray matter), not inside the white matter [11,12]. The brain cortical surface was extracted from an MRI T1 image ($256 \times 256 \times 200$, voxel size for each direction: 1mm) and tessellated into about 500,000 triangular elements including about 250,000 vertices. To extract and tessellate the cortical surface, we used *BrainSuite* developed at the University of Southern California, CA [13]. Then, the lead field matrix in (1) can be

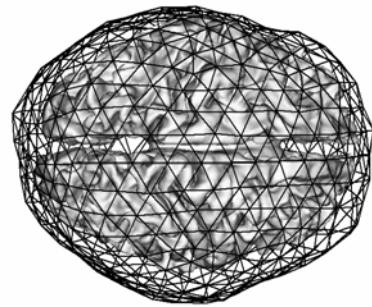


Fig. 1. Boundary element meshes (inner skull boundary). Note that the cortical surface was not included in the boundary element analysis. The cortical surface tessellation was used only for locating the target points and investigating the targeting capability of the simulated magnetic stimulators. In the simulations, the number of cortical surface vertices was diminished to approximately 15,000 to enhance the computational efficiency.

evaluated by assuming unit dipolar sources at each point on the cortical surface and calculating the magnetic field at all coil locations. Fig. 1 shows the boundary element surface meshes co-registered with the tessellated cortical surface.

3. SIMULATIONS AND RESULTS

We performed several simulations for various types and configurations of stimulating coils and investigated the evoked field patterns and targeting accuracy.

3.1. Simulation processes

Before the simulations, the target points should be assumed *a priori*. When a target point is selected among the vertices on the tessellated cortical surface, the evoked field pattern \mathbf{P} in (2) is evaluated. The evoked field pattern vector \mathbf{P} has only nonzero values at the target point. The directions of the targeted electric fields were assumed to be normal to the cortical surface, since the major pyramidal neurons are arranged perpendicularly to the cortical surface [11,12]. The evoked electric field at every cortical vertex was then evaluated using (3).

3.2. Coil configurations

We simulated two types of coil configurations. The proposed 61-channel and 148-channel coils were designed to cover the upper side of a normal human brain. Fig. 2 shows the proposed helmet-type whole head stimulators.

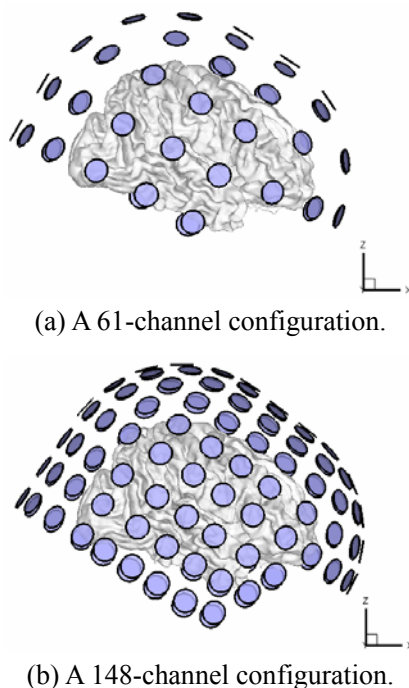


Fig. 2. Configurations of multi-channel stimulating coils.

3.3. Various coil shapes

Conventional stimulating coils that have so far been used for multi-channel TMS were single coils oriented normal to the head surface, as shown in Fig. 3(a) [6]. In the present study, 5 more coil types were simulated, as depicted in Figs. 3(b)-(e).

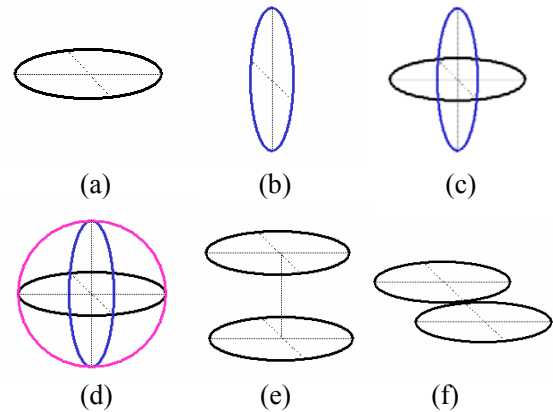


Fig. 3. Various coil types: (a) Type I-normal to head surface; (b) Type II-parallel to head surface; (c) Type III-Type I+Type II; (d) Type IV-Type III + a coil perpendicular to both the Type I and Type II; (e) Type V-same as axial gradiometer in MEG, but operating independently. Distance between two coils=10mm; (f) Type VI-same as planar gradiometer in MEG, but operating independently. (Refer to [8] for the axial and planar gradiometers).

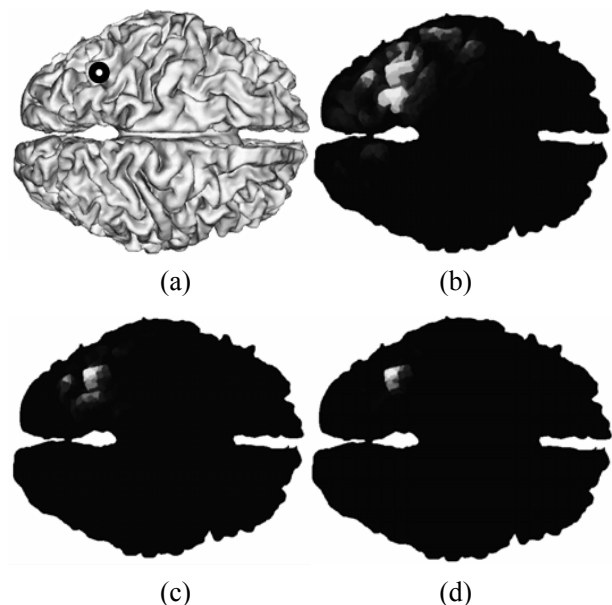


Fig. 4. Distribution of evoked electric fields (current) for the target point marked with a black circle: (a) position of the target point (black circle); (b) result for 61 coils; (c) result for 148 coils; (d) result for 296 coils. The arrows represent the direction of the fields.

3.4. Examples of evoked current distribution

In order to investigate the effect of the number of coils on the field focalization, 61, 148, and 296 coil configurations (148 channel configuration+Type VI coils) were simulated for two test target points. The first target point is presented by a black circle in Fig.

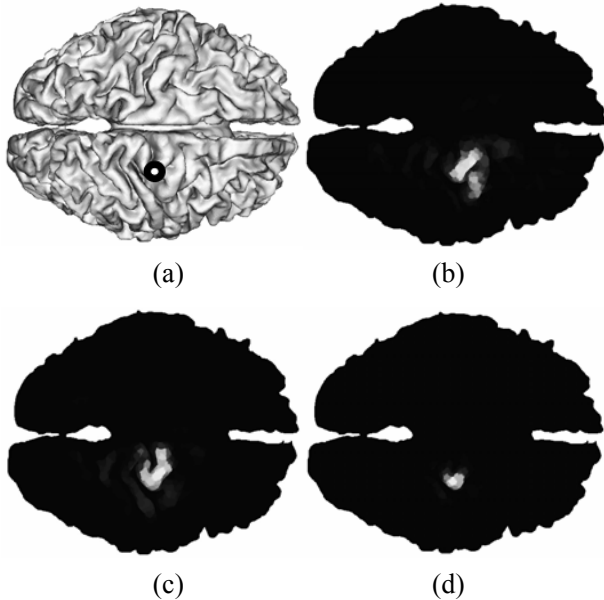


Fig. 5. Distribution of evoked electric fields (current) for a different target point marked with a black circle: (a) position of the target point (black circle); (b) result for 61 coils; (c) result for 148 coils; (d) result for 296 coils. The arrows represent the direction of the fields.

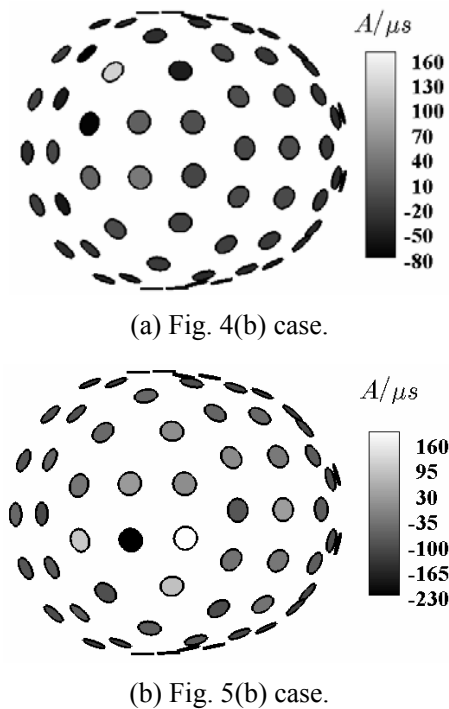


Fig. 6. Examples of current distributions.

4(a). Figs. 4(b), (c), and (d) show the simulation results for the configurations with 61, 148, and 296 coils, respectively. Fig. 5 shows similar simulation results with same configuration as Fig. 4, but target point was different. It can be seen from these results that more focalized field distributions were obtained when the number of stimulating coils was increased. These results seem obvious, since the use of more coils allows more complex and sophisticated electric field patterns to be described, as would be expected. In Fig. 6, the derivatives of the currents in the stimulating coils for Fig. 4(b) and Fig. 5(b) are compared.

3.5. Investigation of targeting accuracy by means of an error map

The most important issue in TMS is to match the maximum point of the evoked current distribution to a target on the cortical surface. In the present study, we first defined an error at the *i*-th node of the cortical surface as the distance between a target point and a maximal point of the evoked current distribution. After evaluating the errors at the entire set of vertices by changing the positions of the target point, we could construct an ‘error map’. This error map can be a useful means of deciding which TMS system is better. Simply by investigating the error map, we could estimate the goodness of a TMS system more intuitively. Fig. 7 shows an error map evaluated for a 61-channel configuration with a Type I coil, in which

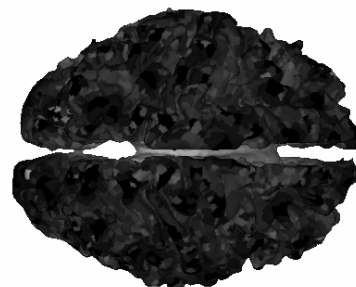


Fig. 7. Error map evaluated for a 61-channel configuration with Type I coil. The brighter region represents the higher error.

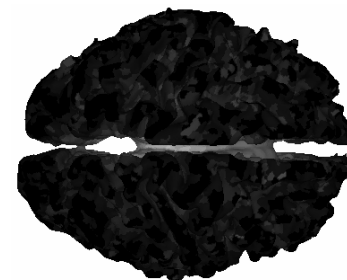


Fig. 8. Error map evaluated for a 61-channel configuration with Type IV coil. The brighter region represents the higher error.

the brighter region represents a higher error. In this figure, it could be observed that the deep brain regions were not well stimulated by the external magnetic stimulations, as was professed in previous studies [1,4]. Fig. 8 illustrates an error map for a 61-channel configuration with a Type IV coil. It can be seen from this figure that the bright regions became smaller compared to those of Fig. 7, which means that type IV has better performance than type I.

To properly elucidate the mechanism of the TMS system, the following three physiological facts need to be considered: (1) The cortical surface is not a flat surface, but a highly folded surface; (2) The cortical pyramidal neurons, which are associated with sensory tasks, are aligned perpendicularly to the cortical surface; (3) The cortical neurons are activated when an electric field is applied parallel to the orientation of the neurons (dendrites).

The conventional one- or two-coil TMS systems only generate electric fields tangential to the scalp or skull surface. Nevertheless, since the cortical surface is highly folded, electric fields applied tangential to the scalp or skull surface can obviously activate some neurons normal to the cortical surface, which are mostly located in sulci regions. Although the suggested multi-channel TMS system can form more complex electric fields, the gyri regions are still difficult to stimulate (see Figs. 7 and 8). Thankfully, most sensory-related neurons are not located on the

gyri, but on the sulci [8].

In practical applications, the targeting errors in the deep regions can be neglected, since current applications of TMS generally concern sensory-related brain activations that occur around shallow cortical areas. Therefore, we excluded the deep points whose depth from the inner skull boundary exceeded 40 mm. The arithmetic mean of the overall errors was then evaluated only at shallow cortical locations.

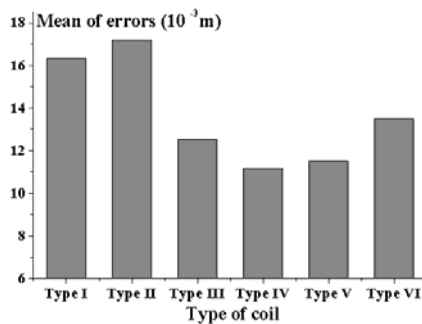
Fig. 9 shows the mean of the targeting errors evaluated with respect to all possible combinations of coil configurations and types. Figs. 9(a) and 9(b) present the results obtained for the 61-channel and 148-channel configurations, respectively.

The results demonstrated that there was not much difference in the accuracy of the type I and type II coils. It is also seen that the type IV coil shows the best performance among all of the coil types considered, but it should be noted that the number of coils used in type IV is three times that of type I. Considering the number of coils used in type IV (1.5 times that of type V), the enhancement in the targeting error does not seem sufficient. Comparing the errors among types III, V, and VI, in which the number of coils is twice that of type I, type V shows better performance than the others. Interestingly, the error of type V is comparable to that of type IV, in spite of the large difference in the number of coils. Moreover, the error of type V in the 61-channel configuration (where the total number of coils is only 122) is even greater than those of type I and type II in the 148-channel configuration. Thus, we can conclude that the type V coil (two axially parallel coils) is the best coil configuration for the multi-channel whole head TMS system.

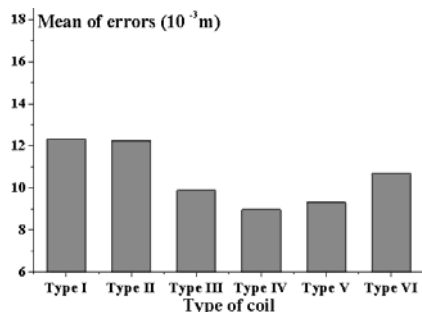
4. CONCLUSIONS

In this paper, we designed a novel whole-head TMS system and simulated various coil types and configurations considering realistic head geometry. The targeting errors with respect to the numbers, configurations, and types of coils were investigated by means of an error map. Several simulation studies demonstrated that the axially parallel coil type stimulator shows the best performance among the various coil types.

Practically, there are some technical difficulties in implementing the proposed multi-channel TMS system, which should be studied in the future. First, to prevent excessive heat generation, the implementation of a cooling system should be considered. Second, the independent operation of multiple stimulating coils requires complex individual circuits, in which the charged voltages should be controllable. Third, mutual inductances between the coils should be considered when designing the external circuit systems [5].



(a) 61-channel configuration.



(b) 148-channel configuration.

Fig. 9. Mean of targeting errors evaluated for all possible types of coil configurations and coil types.

Nevertheless, there is no doubt that the present preliminary design and analysis results can be a useful guide to implement practical multi-channel TMS systems.

REFERENCES

- [1] J. Ruohonen, M. Ollikainen, V. Nikouline, J. Virtanen, and R. J. Ilmoniemi, "Coil design for real and sham transcranial magnetic stimulation," *IEEE Trans. Biomed. Eng.*, vol. 47, pp. 145-148, Feb. 2000.
- [2] J. Starzyński, B. Sawicki, S. Wincenciak, A. Krawczyk, and T. Zyss, "Simulation of magnetic stimulation of the brain," *IEEE Trans. Magn.*, vol. 38, no. 2, pp. 1237-1240, Mar. 2002.
- [3] S. Ueno, "Biomagnetic approaches to studying the brain," *IEEE Eng. Med. Biol.*, vol. 18, pp. 108-120, May/June 1999.
- [4] J. Ruohonen, P. Ravazzani, F. Grandori, and R. J. Ilmoniemi, "Theory of multichannel magnetic stimulation: Toward functional neuromuscular rehabilitation," *IEEE Trans. Biomed. Eng.*, vol. 46, no. 6, pp. 646-651, Jun. 1999.
- [5] B.-H. Han, I.-K. Chun, S.-C. Lee, and S.-Y. Lee, "Multi-channel magnetic stimulation system design considering mutual couplings among the stimulation coils," *IEEE Trans. Biomed. Eng.*, vol. 51, pp. 812-817, 2004.
- [6] J. Ruohonen and R. J. Ilmoniemi "Focusing and targeting of magnetic brain stimulation using multiple coils," *Med. Biol. Eng. Comput.*, vol. 36, pp. 297-301, May 1998.
- [7] F. Binkofski, J. Classen, and R. Benecke, "Stimulation of peripheral nerves using a novel magnetic coil," *Muscle Nerve*, vol. 22, pp. 751-757, 1999.
- [8] M. S. Hämäläinen, R. Hari, R. J. Ilmoniemi, J. Knuutila, and O. V. Lounasmaa, "Magnetoencephalography. Theory, instrumentation and applications to the noninvasive study of human brain function," *Rev. Mod. Phys.* vol. 65, pp. 413-497, 1993.
- [9] M. S. Hämäläinen and J. Sarvas, "Realistic conductivity geometry model of the human head for interpretation of neuromagnetic data," *IEEE Trans. Biomed. Eng.*, vol. 36, pp. 165-171, 1989.
- [10] J. W. Meijs, M. J. Peters, H. B. Boom, and F. H. Lopes da Silva, "Relative influence of model assumptions and measurement procedures in the analysis of the MEG," *Med. Biol. Eng. Comput.*, vol. 26, pp. 136-142, 1988.
- [11] C.-H. Im, H.-K. Jung, and N. Fujimaki, "fMRI constrained MEG source imaging and consideration of fMRI invisible sources," *Hum. Brain Mapp.*, vol. 26, no. 2, pp. 110-118, 2005.
- [12] A. M. Dale and M. Sereno, "Improved localization of cortical activity by combining EEG and MEG with MRI surface reconstruction: A linear approach," *J. Cognit. Neurosci.*, vol. 5, pp. 162-76, 1993.
- [13] D. W. Shattuck and R. M. Leahy, "BrainSuite: An automated cortical surface identification tool," *Med. Image. Anal.*, vol. 6, pp. 129-142, 2002.



Chany Lee was born in Taegu, Korea in 1980. He graduated from the school of Electrical Engineering, Seoul National University in 2003. He received the M.S. from the same university in 2005. He is now working toward a Ph.D. in the School of Electrical Engineering and Computer Science of Seoul National University.

His research interests are bioelectromagnetics and transcranial magnetic stimulation.



Chang-Hwan Im graduated from the School of Electrical Engineering, Seoul National University in 1999. He received the M.S. and Ph.D. at the same university in 2001 and 2005, respectively. He worked as a Post-doctoral Associate at the Department of Biomedical Engineering, University of Minnesota, MN, USA, from 2005 to

2006. From 2006, he is working as an Assistant Professor at the Department of Biomedical Engineering, Yonsei University, Korea. His research interests cover various fields of bioelectromagnetics, especially bioelectromagnetic source imaging, EEG/MEG/MCG forward/inverse problems, transcranial magnetic stimulation, etc.



Hyun-Kyo Jung graduated from the School of Electrical Engineering, Seoul National University in 1979. He received the M.S and Ph.D. at the same university in 1981 and 1984, respectively. He worked as a Faculty at Kangwon National University from 1985 to 1994 and joined the Polytechnic University in New York,

USA, in 1987 where he remained until 1989. He has been teaching at Seoul National University since 1994. From 1999 to 2000, he also served as a Visiting Professor in UC Berkley, USA. His research interests cover the various fields of the analysis and design of electric machinery and numerical field analysis of electrical systems, especially with the Finite Element Method.